



HAL
open science

Anomalous flow below 2700 m in the EPICA Dome C ice core detected using d18O of atmospheric oxygen measurements

G. B. Dreyfus, F. Parrenin, B. Lemieux-Dudon, Geoffroy Durand, Valérie Masson-Delmotte, Jean Jouzel, J.-M. Barnola, L. Panno, R. Spahni, A. Tisserand, et al.

► To cite this version:

G. B. Dreyfus, F. Parrenin, B. Lemieux-Dudon, Geoffroy Durand, Valérie Masson-Delmotte, et al.. Anomalous flow below 2700 m in the EPICA Dome C ice core detected using d18O of atmospheric oxygen measurements. *Climate of the Past*, 2007, 3 (2), pp.341-353. 10.5194/CP-3-341-2007. hal-00330756

HAL Id: hal-00330756

<https://hal.science/hal-00330756>

Submitted on 18 Jun 2008

HAL is a multi-disciplinary open access archive for the deposit and dissemination of scientific research documents, whether they are published or not. The documents may come from teaching and research institutions in France or abroad, or from public or private research centers.

L'archive ouverte pluridisciplinaire **HAL**, est destinée au dépôt et à la diffusion de documents scientifiques de niveau recherche, publiés ou non, émanant des établissements d'enseignement et de recherche français ou étrangers, des laboratoires publics ou privés.



Distributed under a Creative Commons Attribution 4.0 International License

Anomalous flow below 2700 m in the EPICA Dome C ice core detected using $\delta^{18}\text{O}$ of atmospheric oxygen measurements

G. B. Dreyfus^{1,2}, F. Parrenin³, B. Lemieux-Dudon³, G. Durand⁴, V. Masson-Delmotte¹, J. Jouzel¹, J.-M. Barnola³, L. Panno⁵, R. Spahni⁵, A. Tisserand⁶, U. Siegenthaler⁵, and M. Leuenberger⁵

¹LSCE/IPSL, CEA-CNRS-UVSQ, CE Saclay, 91191, Gif-sur-Yvette, France

²Department of Geosciences, Princeton University, Princeton, New Jersey, USA

³Laboratoire de Glaciologie et Geophysique de l'Environnement (CNRS), St Martin d'Herès, France

⁴Niels Bohr Institute for Astronomy, Physics and Geophysics, University of Copenhagen, Copenhagen, Denmark

⁵Physics Institute, University of Bern, Bern, Switzerland

⁶Université Bordeaux I, UMR 5805 EPOC, Environnements et Paléoenvironnements Océaniques et Côtiers, Talence Cedex 33405, France

Received: 20 November 2006 – Published in *Clim. Past Discuss.*: 16 January 2007

Revised: 15 May 2007 – Accepted: 5 June 2007 – Published: 21 June 2007

Abstract. While there are no indications of mixing back to 800 000 years in the EPICA Dome C ice core record, comparison with marine sediment records shows significant differences in the timing and duration of events prior to stage 11 (~430 ka, thousands of years before 1950). A relationship between the isotopic composition of atmospheric oxygen ($\delta^{18}\text{O}$ of O_2 , noted $\delta^{18}\text{O}_{\text{atm}}$) and daily northern hemisphere summer insolation has been observed for the youngest four climate cycles. Here we use this relationship with new $\delta^{18}\text{O}$ of O_2 measurements to show that anomalous flow in the bottom 500 m of the core distorts the duration of events by up to a factor of 2. By tuning $\delta^{18}\text{O}_{\text{atm}}$ to orbital precession we derive a corrected thinning function and present a revised age scale for the interval corresponding to Marine Isotope Stages 11–20 in the EPICA Dome C ice core. Uncertainty in the phasing of $\delta^{18}\text{O}_{\text{atm}}$ with respect to insolation variations in the precession band limits the accuracy of this new agescale to ± 6 kyr (thousand of years). The previously reported ~30 kyr duration of interglacial stage 11 is unchanged. In contrast, the duration of stage 15.1 is reduced by a factor of 2, from 31 to 16 kyr.

C. This approximation, however, does not always hold, as evidenced by the disturbances in the bottom of the Summit Greenland ice cores (Fuchs and Leuenberger, 1996; Grootes et al., 1993).

The recent recovery of the 3260 m EPICA Dome C (EDC) ice core extends the available Antarctic ice core record to 8 climate cycles (EPICA community members, 2004; Parrenin et al., 2007a). The previous EDC chronology, named EDC2, was derived using a one-dimensional glaciological model with optimised parameters determined with an inverse modelling approach using 5 chronological controls tied to marine records for the period before 50 ka (thousand of years before 1950) (EPICA community members, 2004). This modelling approach provides consistent reconstructions of the accumulation rate history and the mechanical strain imposed thinning profile, such that the age at a given depth z can be calculated as follows:

$$A(z) = \int_0^z \frac{1}{T(z')a(z')} dz' \quad (1)$$

Intuitively, the age A at a given depth z is equal to the sum from the surface to z of the inverse of the annual layer thicknesses, which are given by the accumulation rate a at the time of deposition adjusted by the thinning function T that incorporates the physical flow effects related to variations in ice sheet surface elevation and basal melting and sliding.

Overall, the temperature record derived from the deuterium (δD) content of the ice is in excellent agreement with the LR04 marine benthic stack back to 800 ka (Lisiecki and Raymo, 2005), indicating that EDC preserves correct stratigraphy through at least 740 ka. Mixing can be discounted due to the absence of abrupt changes in both ice and gas parameters in the same depth interval that are characteristic of

1 Introduction

The physical constraints on ice accumulation and flow make it possible to derive ice timescales using glaciological models. One-dimensional models are generally deemed appropriate for cores drilled on ice domes, such as EPICA Dome

Correspondence to: G. B. Dreyfus
(gabrielle.dreyfus@cea.fr)

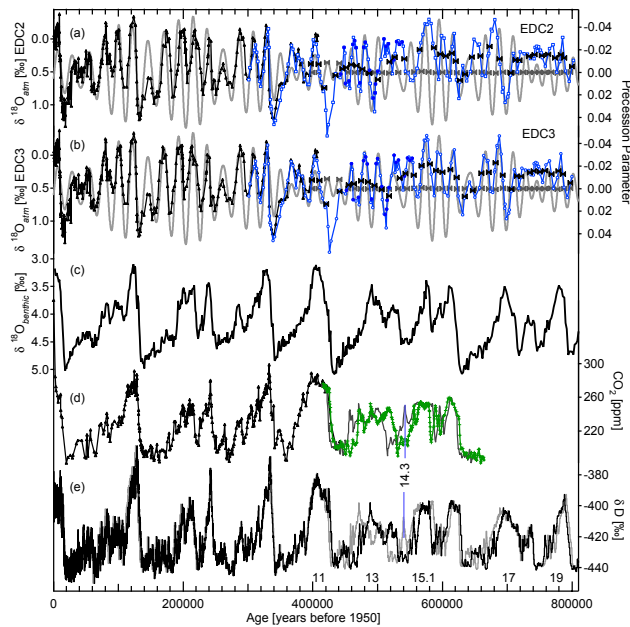


Fig. 1. Orbital and climatic profiles since 800 ka: **(a)** $\delta^{18}\text{O}_{\text{atm}}$ records from Vostok (triangles; Petit et al., 1999) on the FGT1 timescale (Parrenin et al., 2004) and EDC in blue (open squares LSCE, filled squares UNIBE) on the EDC2 timescale (EPICA community members, 2004), and the precession parameter shifted younger by 5 kyr (Laskar, 2004); **(b)** as in (a), but with Vostok and EDC $\delta^{18}\text{O}_{\text{atm}}$ plotted on the new EDC3 tuned timescale (this work and Parrenin et al., 2007b); **(c)** LR04 marine benthic stack on its own timescale (Lisiecki and Raymo, 2005); **(d)** CO₂ record from Vostok (triangles; Petit et al., 1999) and EDC (Siegenthaler et al., 2005) on EDC2 (grey) and EDC3 (green crosses); **(e)** EDC deuterium on EDC2 (light grey) and EDC3 (black). Bow-ties on the precession and $\delta^{18}\text{O}_{\text{atm}}$ profiles represent the age control points used in determining the optimised chronology.

the mixing observed at the bottom of the Greenland Summit cores (Fuchs and Leuenberger, 1996; Landais et al., 2003b; Suwa et al., 2006) and in the Vostok core (Raynaud et al., 2005). Environmental changes affecting both gases and temperature are recorded at greater ice depth in the core for the δD -derived temperature than for the gas phase. This is a consequence of the gas enclosure processes that occur approximately 100 m below the surface of the ice sheet at EDC. This is indeed the case for the CO₂ (Siegenthaler et al., 2005) and CH₄ (Spahni et al., 2005) concentrations measured in EDC back to 650 ka, and additional measurements show the expected depth offset through the end of stage 20.

Closer comparison between the EDC isotopic record and the LR04 marine stack (Lisiecki and Raymo, 2005) suggests problems with the duration of events in the EDC2 chronology over the interval covering Marine Isotope Stages (MIS) 12–15, roughly 430 to 630 ka, corresponding to 2780–3040 m depth in the core (Fig. 1). The authors of the stack noted that to match EDC2 over MIS 12–15 would require spuri-

ous fluctuations in the normalised sedimentation rate of the over 30 cores covering this interval. Similarly, matching to EDC2 over stages 16 and 17 required small variations in the sedimentation rate. If we consider that normalised sedimentation rate is a stringent constraint on the marine stack age scale, then the source of the disaccord must be due to problems in the EDC2 chronology. Further evidence of problems with the EDC2 agescale over this period comes from sedimentation rate estimates at ODP Site 1093 in the Southern Ocean that are in conflict with the overall pattern in biogenic opal deposition when the EDC2 age scale is applied (R. Gersonde, personal communication, 2006). These comparisons with marine records suggest that EDC2 overestimates the duration of the interval representing MIS 14 and 15.1 by about a factor of two.

There are two possible causes for distortion of the duration of events in EDC over the bottom 500 m of the core: i) the accumulation rate parameterisation as a function of δD content (Jouzel et al., 1987) differs for this period, or ii) the 1-D mechanical flow model fails to capture the physical processes operating on the bottom 500 m of the ice.

While trace gases permit the integrity of core stratigraphy to be verified on a local scale, the isotopic composition of atmospheric oxygen ($\delta^{18}\text{O}$ of O₂, noted $\delta^{18}\text{O}_{\text{atm}}$) provides a pacemaker for large scale chronology evaluation as a consequence of its strong coherence with northern hemisphere summer insolation variations in the precession band, as shown in the Vostok record for the last four climatic cycles (Petit et al., 1999). The temporal variations in $\delta^{18}\text{O}_{\text{atm}}$ on the order of 1‰ depend on ice volume, the hydrological cycle and on the activities of the marine and terrestrial biospheres (Sowers et al., 1991). Ice volume and the hydrological cycle control the isotopic composition of oxygen in water, a signal that is transferred to the atmosphere via photosynthesis and respiration with distinct isotopic signatures for the marine and terrestrial realms (Bender et al., 1994b). Modulation of the monsoon by precession of the equinoxes affects activity of the terrestrial biosphere and humidity, and has been linked to variations in $\delta^{18}\text{O}_{\text{atm}}$ (Hoffmann et al., 2004; Leuenberger, 1997; Malaizé et al., 1999). While $\delta^{18}\text{O}_{\text{atm}}$ is an useful chronological tool (Bender, 2002), its precision is limited by uncertainties in the processes controlling its phasing with respect to insolation forcing. Previous authors have assumed an uncertainty of ± 6 kyr, equivalent to half a precession cycle and the extrema in phase with respect to 21 June 65° N insolation on the Vostok Extended Glaciological Timescale (Jouzel et al., 1996). This uncertainty estimate based on mechanistic assumptions has been empirically supported by the improved Vostok FGT1 chronology (Parrenin et al., 2004).

Here we present the first measurements of the isotopic composition of atmospheric oxygen extracted from the EDC ice core. Assuming that similar mechanisms are at play prior to 400 ka, we exploit the relationship between $\delta^{18}\text{O}_{\text{atm}}$ and precession to provide additional evidence of a problem with

the duration of events in the bottom 500 m of EDC. Several observations including the phase between climate records in the gas and ice phases allow us to distinguish between accumulation rate and thinning as the source of the observed perturbation. Finally, we propose a revised chronology using age control points derived from orbital tuning of $\delta^{18}\text{O}$ of O₂ with precession.

2 Methods and measurements

2.1 Measurements of $\delta^{18}\text{O}_{\text{atm}}$

The isotopic composition of trapped air from the EPICA Dome C core (75°06' S; 123°21' E; 3233 m above sea level) was measured at the Laboratoire des Sciences du Climat et de l'Environnement (LSCE), France, and the Climate and Environmental Physics Institut of the University of Bern (UNIBE), Switzerland. In total, measurements from 170 depth levels between 2482.7 and 3191.1 m are reported giving a mean depth resolution of 4.2 m, with 147 LSCE measurements and 23 UNIBE measurements. An additional 41 data points are presented between 357.3 and 572.3 m, covering the last deglaciation, measured at LSCE in 2003. The UNIBE samples are measured using an on-line continuous flow technique fully described elsewhere (Huber and Leuenberger, 2004; Huber et al., 2003). Mean error for UNIBE $\delta^{18}\text{O}_{\text{atm}}$ is 0.03‰, and is calculated by dividing the standard deviation of the raw values by the square root of the measurement duration (ranging between 142 and 901 s). Samples measured at LSCE were processed using a melt-refreeze method with 183 samples from 88 depths analyzed on a Finnigan MAT 252 isotope ratio mass spectrometer in 2004–2005, and 126 samples from 59 depths were measured in 2006 using the same extraction procedure but a new Delta V Plus (Thermo Electron Corporation) mass spectrometer equipped with 10-cups permitting simultaneous acquisition of $m/z=28, 29, 30, 32, 33, 34, 36, 38, 40$ and 44. The LSCE analytical method is described in detail in Landais et al. (2003a). Briefly, the trapped air is extracted by melting ~10 g samples under vacuum. The water is then refrozen, and the gases remaining in the headspace are cryogenically trapped in a steel tube at liquid He temperature. On the Finnigan MAT 252, dual detector measurements for $^{15}\text{N}/^{14}\text{N}$ (actually m/z ratio 29/28) and $^{18}\text{O}/^{16}\text{O}$ (m/z ratio 34/32) were made in sequential runs. Corrections are applied for pressure imbalance and chemical interference for all measurements. The working standard (ST2) is dried exterior lab air collected in 1998 stored in a 3-litre stainless steel canister. The standard is calibrated against 3 cm³ STP of dried exterior air twice a week. All results are reported with respect to atmospheric air. Each depth was measured at least twice, and the pooled standard deviation for replicate measurements at LSCE yielded precisions of 0.011‰ (0.004‰ on the Delta V Plus) and 0.04‰ (0.028‰ on the Delta V Plus) for $\delta^{15}\text{N}$ and

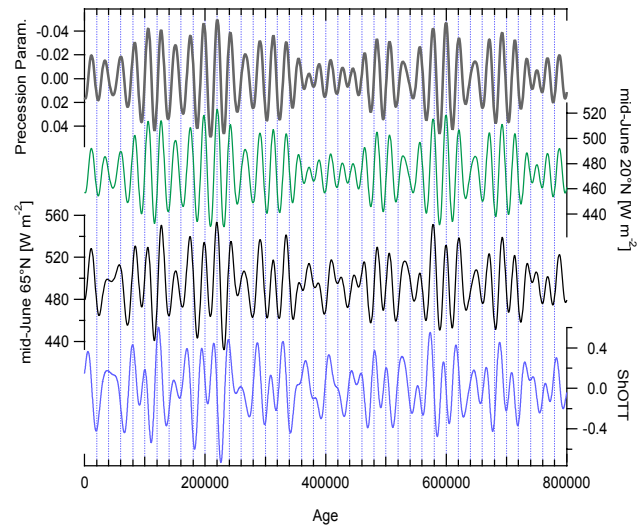


Fig. 2. Previous studies have compared variations in $\delta^{18}\text{O}_{\text{atm}}$ to the various insolation curves shown here. From top to bottom: the precession parameter ($p=e \sin \varpi$) used in this study, mid-June insolation at 20° N (Malaizé et al., 1999), mid-June insolation at 65° N (Jouzel et al., 1996; Petit et al., 1999), and the Shackleton (2000) tuning target (ShOTT) a combination of obliquity and precession adjusted to match the phase and amplitude for each band in the Vostok $\delta^{18}\text{O}_{\text{atm}}$ record. All orbital curves have been calculated with the Analyseries 2.0.3.2 software (Paillard et al., 1996) using the Laskar et al. (2004) solution.

$\delta^{18}\text{O}_{\text{atm}}$, respectively. $\delta^{18}\text{O}_{\text{atm}}$ is defined as $\delta^{18}\text{O} - 2 \times \delta^{15}\text{N}$; it is the $\delta^{18}\text{O}$ of paleoatmospheric O₂ after correction for gravitational fractionation in the firm.

2.2 Orbital tuning

Visible inspection of panel (a) in Fig. 1 reveals the strong similarity between cyclical variations in $\delta^{18}\text{O}_{\text{atm}}$ and variations in the precession of the Earth's orbit. The significant correlation between $\delta^{18}\text{O}$ of O₂ and mid-June 65° N insolation (Jouzel et al., 1996) has prompted several workers to derive ice core chronologies assuming either that the mid-slope of a $\delta^{18}\text{O}_{\text{atm}}$ transition occurs at the same time as the mid-June 65° N insolation maxima as for the last termination (Petit et al., 1999) or a constant phase relationship between $\delta^{18}\text{O}_{\text{atm}}$ and an insolation curve, e.g. mid-June 65° N (Jouzel et al., 1996; Petit et al., 1999) or integrated June 20° N (Bender et al., 1994b) or mid-June 20° N (Malaizé et al., 1999). In order to make use of the strong amplitude modulation of the precession signal and to avoid a specific insolation curve, Shackleton (2000) constructed a tuning target, referred to here as ShOTT, that combines obliquity and precession components shifted and scaled to their respective lags and amplitudes in the filtered Vostok $\delta^{18}\text{O}_{\text{atm}}$ record. Four of these reference curves are shown in Fig. 2: the precession parameter (defined as $p=e \sin \varpi$ where e is the orbital eccentricity

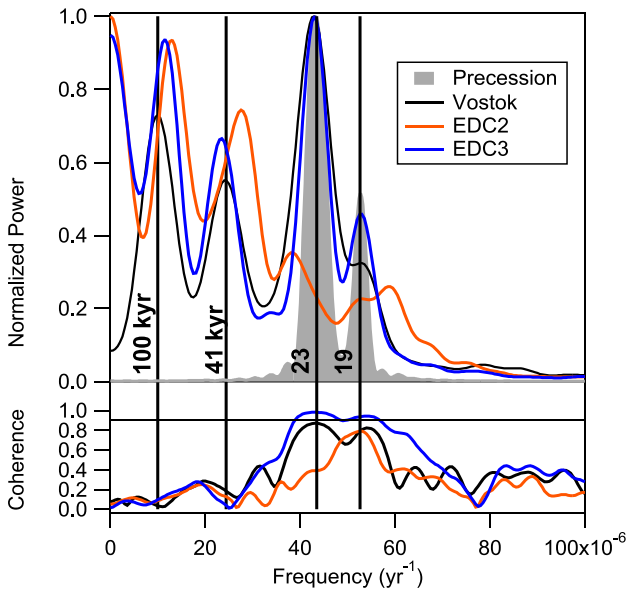


Fig. 3. Spectral properties of the precession parameter (solid grey) and $\delta^{18}\text{O}_{\text{atm}}$ from Vostok (black; Petit et al., 1999) on the FG1 timescale (Parrenin et al., 2004) and from EDC (this study) on the EDC2 (red; EPICA community members, 2004) and tuned EDC3 (blue; this study). Coherency of each record with respect to the precession parameter is shown in the bottom panel. The horizontal line indicates 90% significance level. Analysis was done with the Blackman-Tukey method using the AnalyseSeries software (Paillard et al., 1996).

and ϖ is the angle of the perihelion with respect to the vernal point), mid-June 20° N insolation, mid-June 65° N insolation, and the ShOTT tuning target (Shackleton, 2000). Note that the influence of obliquity increases from the top to bottom panel, and that the phasing of the top three curves are very similar, whereas the phasing has been shifted by 5 kyr and 3 kyr for the precession and obliquity bands, respectively, in ShOTT.

Here we choose to compare the $\delta^{18}\text{O}_{\text{atm}}$ record with the precession parameter rather than with a specific insolation curve to focus specifically on the precession component of variation. Precession, the timing of the seasons with respect to perihelion, has a strong effect on the amplitude of the seasons and on monsoon intensity in particular (Prell and Kutzbach, 1987). Variations in $\delta^{18}\text{O}_{\text{atm}}$ have been linked to this modulation of the monsoons via associated changes in the hydrological cycle and terrestrial biospheric activity (Malaizé et al., 1999). The precession parameter is calculated using the Laskar et al. (2004) orbital solution with the AnalyseSeries 2.0.3.2 software (Paillard et al., 1996). The chosen definition of precession parameter is negative when insolation due to precession is increasing in the northern hemisphere. Since $\delta^{18}\text{O}_{\text{atm}}$ has been shown to be coherent with insolation variations in the northern hemisphere (Bender, 2002), we consider the precession parameter on a re-

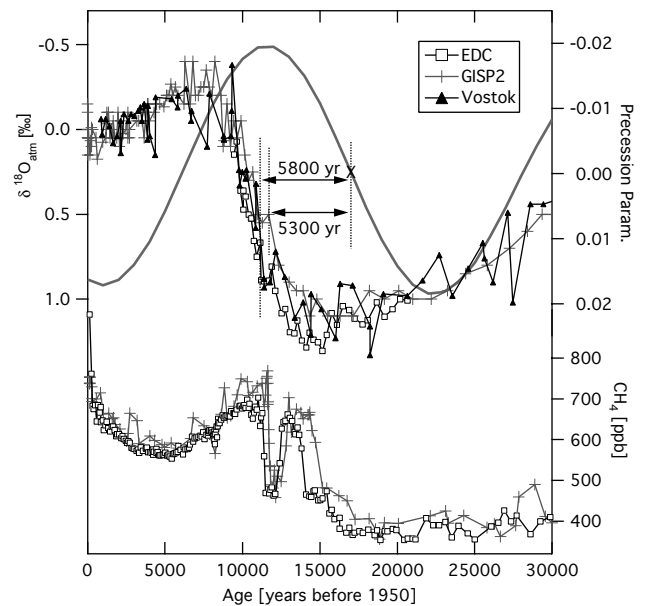


Fig. 4. Phasing between variations in the precession parameter (solid grey line) and $\delta^{18}\text{O}_{\text{atm}}$ over the most recent transition, with EDC data shown with open squares (this study), Vostok data with filled triangles (Petit et al., 1999) and GISP2 data with dark grey crosses (Bender et al., 1994a; Sowers et al., 1997). Methane from EDC (Monnin et al., 2001) and GISP2 (Brook et al., 1996) is shown for chronological context and comparison. All EDC data is plotted on the EDC3 chronology, Vostok data on FG1 (Parrenin et al., 2004) and GISP2 data on the Meese/Sowers chronology (Meese et al., 1994). All GISP2 data provided by the National Snow and Ice Data Center, University of Colorado at Boulder, and the WDC-A for Paleoclimatology, National Geophysical Data Center, Boulder, Colorado.

versed scale. We note that by considering only precession, we ignore the significant obliquity component in the Vostok $\delta^{18}\text{O}_{\text{atm}}$ record (Fig. 3). The implications of this choice are assessed by independently tuning to ShOTT, which has equal power in the 1/41 and 1/23 kyr⁻¹ bands.

For the purposes of the orbital tuning presented here, we have assumed a constant phase lag between $\delta^{18}\text{O}_{\text{atm}}$ and the precession parameter. Following Shackleton (2000), this lag can most accurately be assessed by looking at the timing for the most recent and best-dated transition in $\delta^{18}\text{O}_{\text{atm}}$, which occurred between roughly 14.6 and 8.6 ka, with a mid-point around 11.5 ka (Fig. 4). The mid-point of the transition in mid-June 65° N insolation and the precession parameter occurred at 17 ka. By virtue of the layers present in Greenland records available for counting and the much smaller gas age-ice age differences (several hundred years in Greenland compared to several thousand in central Antarctica), we consider the Greenland agescales to be the most precise, with the new multiparameter GICC05 chronology (Rasmussen et al., 2006) confirming the GISP2 dating to within 100 years between 8 and 15 ka. For this reason we adopt a constant

Table 1. Age control points for the optimised chronology (years before 1950).

Tie-Point Depth [m]	Precession Age (–5 kyr)	EDC3 Δage	Tie-Point Ice Age
2707.65			398 095
2714.32	398 396	2144	400 540
2749.04	408 621	2001	410 622
2772.27	422 036	2461	424 498
2799.36	440 995	4620	445 615
2812.69	454 294	4864	459 158
2819.2	464 557	4802	469 358
2829.36	474 756	3621	478 377
2841.75	485 293	2913	488 206
2856.27	495 921	3125	499 046
2872.56	506 642	3617	510 259
2890.33	517 602	3027	520 630
2913.3	532 027	4196	536 224
2921.99	545 313	4547	549 860
2938.24	556 414	3454	559 869
2968.08	567 606	2569	570 175
2998.96	578 627	3317	581 944
3008.93	589 460	3467	592 927
3017.25	600 078	3434	603 512
3027.54	610 875	2424	613 299
3035.41	622 074	2703	624 777
3043.01	634 419	5033	639 452
3048.51	649 064	4404	653 468
3056.77	660 789	4731	665 520
3065.93	671 703	4440	676 142
3077.74	682 326	3608	685 934
3093.51	693 159	2628	695 787
3112.43	703 964	3106	707 070
3119.57	714 369	3385	717 754
3124.27	724 376	4080	728 456
3136.18	733 949	3298	737 247
3143.2	741 944	5055	747 000
3152.25	749 184	4860	754 044
3158.91	758 069	4027	762 096
3166.87	767 679	3562	771 241
3174.81	777 607	2769	780 377
3180.6	787 736	2399	790 135
3189.83	797 460	4979	802 439

phase lag of 5000 years, closer to the observed GISP2 age, as did Shackleton (2000). It should be noted that the last deglaciation is peculiar in its sequence of interruptions by the Bølling-Allerød/Younger Dryas and Antarctic Cold Reversal, which may impact the inferred phasing. It is, however, the best available constraint. We applied a similar procedure of identifying mid-points in the precession parameter curve and the Vostok $\delta^{18}\text{O}_{\text{atm}}$ record (Petit et al., 1999) on the improved FGT1 age scale (Parrenin et al., 2004), and found a mean phasing of 5.8 ± 1.6 kyr with a range of 3–10 kyr. That the phase between $\delta^{18}\text{O}_{\text{atm}}$ and precession is not constant within several thousand years is expected given the numerous and complex processes influencing the response of $\delta^{18}\text{O}$

of air to changes in seawater $\delta^{18}\text{O}$ and biospheric activity (Bender et al., 1994b; Hoffmann et al., 2004; Jouzel et al., 2002; Leuenberger, 1997; Malaizé et al., 1999; Parrenin et al., 2001). For example, changes in biospheric carbon inventory during glacial and interglacial periods imply changes in oxygen flux and reservoir age (Leuenberger, 1997). Without a mechanistic understanding of these processes, however, we cannot predict how the response time varied, and for this reason assume a constant phase lag and assign a conservative 3 kyr Gaussian 1σ uncertainty based on analysis of the Vostok record and modelling studies (Hoffmann et al., 2004; Leuenberger, 1997).

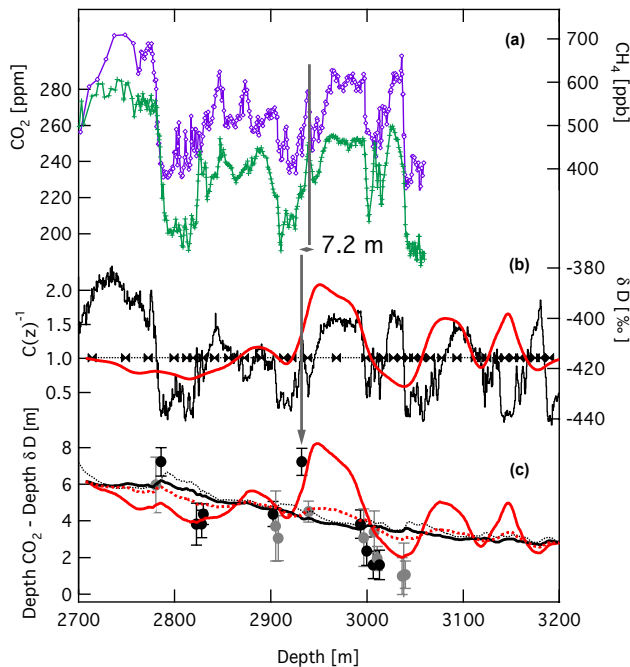


Fig. 5. (a) Measured CO₂ (green crosses; Siegenthaler et al., 2005) and CH₄ (purple diamonds; Spahni et al., 2005) plotted against depth. (b) Inverse of the derived correction factor (red) shown with the δD profile and tie-points (bow-ties). Values of $C(z)^{-1}$ greater than 1 contract the original expected agescale (equivalent to an increased accumulation rate or stretched ice interval). (c) Comparison of observed CO₂ depth- δD depth (circles shaded according to confidence, where lighter values are more uncertain) with modelled Δ depth calculated as the product of the densified lock-in-depth and thinning (T). The untuned EDC2 (thin dotted) and EDC3 (thick black) modelled Δ depths are compared with the tuned EDC3 assuming anomalous T (solid red) and anomalous accumulation (dotted red).

To reduce errors associated with identifying extrema in a low-resolution record, we choose 33 tie points on the mid-slopes and 2 tie-points on shoulders or inflections during a period of combined strong ice volume signal over MIS 12 to 11 and low precession variability (Table 1 and Fig. 1). Ideally, such orbital tuning should be done with $\delta^{18}\text{O}_{\text{atm}}$ corrected for the ice volume signal by subtracting the appropriate seawater oxygen-18 profile. Separating local hydrographic and temperature effects from the ice volume signal in $\delta^{18}\text{O}_{\text{benthic}}$, however, is a complex task. Recently Bintanja et al. (2005) deconvoluted the LR04 benthic isotope stack (Lisiecki and Raymo, 2005) to isolate an ice volume component. We find that subtracting this profile from our EDC $\delta^{18}\text{O}_{\text{atm}}$ record (after matching to account for EDC agescale distortion) does not appreciably improve the tuning profile, but rather adds sharp variations presumably due to dating and deconvolution uncertainties.

The precession period is 22–23 kyr according to spectral analysis, so we choose 2 tie-points per cycle, every ~ 11 kyr.

We have repeated the correlation using the tuning target derived by Shackleton (2000). Age controls using each tuning target differ by no more than 3 kyr and on average indicate older marker ages by 0.6 kyr using the ShOTT target.

Since these age controls are derived from $\delta^{18}\text{O}_{\text{atm}}$, which is in the gas phase, they must be corrected for the gas age – ice age difference (Δ age) to be transferred to the ice chronology. As shown in Table 1, we use the EDC3 model Δ ages, calculated using a firn densification model (Goujon et al., 2003). The uncertainty in the Δ age evaluation ($1\sigma=0.5$ kyr at maximum) is already included in the 3 kyr uncertainty described above.

2.3 Δ depth markers

The age difference between the trapped gas and the ice (Δ age) is a function of the ice-equivalent lock-in depth (LID) divided by the accumulation rate. The in-situ depth separating gas from ice of the same age (Δ depth), in contrast, is equal to the ice-equivalent LID multiplied by the amount of thinning the intervening ice layer has undergone. The Δ age and LID can be calculated with a firn densification model (Goujon et al., 2003), where we use a factor of 0.7 to convert to ice equivalent depth. For EDC, the LID varies by less than 20% over 800 kyr, thus Δ age is primarily a function of accumulation rate and Δ depth a function of thinning. In calculating the modelled Δ depth, we assume a 10% uncertainty in both the modelled LID and thinning function. By identifying ice and gas markers of the same age and comparing with the modelled Δ depth, it should then, in principle, be possible to estimate the total thinning function at these depths and to distinguish between the two possible sources of an age-scale distortion.

The observed depth differences (Δ depths) between ice δD content and CO₂ concentration (Siegenthaler et al., 2005) for 23 events have been calculated (Fig. 5). The selected points are assigned different confidence ranks depending on the ease of identification of events in each record (Table 2). Glacial inceptions have been avoided, as CO₂ tends to decrease during glacial inceptions after δD content (Cuffey and Vimeux, 2001). Uncertainty in observed Δ depth is determined by the sample resolution and ability to identify the depth of the selected feature. For the purposes of this study, we have assumed that δD content and CO₂ vary in phase for the selected events. It should be noted that the CO₂ concentration increase appears to lag slightly the increase in δD ratio of the ice by 800 ± 600 years at the start of the last glacial termination (Monnin et al., 2001). Studies of the Vostok record found similar lags of around 1000 years at the start of glacial terminations (Caillon et al., 2003; Fischer et al., 1999; Petit et al., 1999). One exception to the exclusion of early glaciations is the minimum before 14.3, which occurs during the early cooling phase between interglacial 15 and glacial stage 14. We may underestimate the Δ depth separating ice and gas of the same age for this event by assuming synchronicity.

Table 2. Selected markers for observed depths separating synchronous changes in CO₂ concentration (Siegenthaler et al., 2005) and deuterium content of ice (temperature proxy). Default uncertainty in depth attribution for δD is 0.55 m, equivalent to bag resolution.

	Event	δD depth	δD uncert	CO ₂ depth	CO ₂ uncert	Δ depth	Δ depth Uncertainty	Confidence
		[m]	[m]	[m]	[m]	[m]	[m]	
TV	end TV	2775.3	0.55	2780	0.5	4.7	0.74	Low
	st-end/2	2780.525	1.1	2786.485	1.05	5.96	1.52	Mid
	start-TV	2785.75	0.55	2792.97	0.55	7.22	0.78	High
Stage 12	MIS 12.5	2822.6	0.55	2826.42	1	3.82	1.14	High
	MIS 12.7	2828.1	0.275	2831.93	0.7	3.83	0.75	High
	MIS 12.8	2829.75	0.275	2834.12	0.5	4.37	0.57	High
Stage 13	spike on 13.1	2842.4	0.275	2847.7	0.36	5.3	0.45	Low
TVI	end-TVI	2902.35	0.55	2906.72	0.4	4.37	0.68	High
	st-end/2	2904.975	1.1	2908.69	0.95	3.715	1.91	Mid
	start-TVI	2907.6	1.1	2910.66	0.55	3.06	1.23	Mid
Stage 14	MIS 14.3	2932.05	0.55	2939.27	0.5	7.22	0.74	High
	start	2939.2	0.275	2943.7	0.5	4.5	0.57	Low
Stage 15.1	end	2993.1	0.55	2996.92	0.55	3.82	0.78	High
	st-end/2	2996.4	1.1	2999.485	1.1	3.085	1.56	Mid
	start	2999.7	0.55	3002.05	0.55	2.35	0.78	High
Stage 15.3	MIS 15.3 A	3006.3	0.55	3007.9	0.5	1.6	0.74	High
	MIS 15.3 B	3007.4	0.55	3010.8	1	3.4	1.14	Mid
	MIS 15.3 C	3010.7	0.55	3012.65	0.35	1.95	0.65	Mid
	MIS 15.3 D	3012.9	0.55	3014.5	0.6	1.6	0.81	High
TVII	end-TVII	3036.6	0.55	3037.6	0.85	1	1.01	Mid
	st-end/2	3038.225	1.1	3039.26	1.35	1.035	1.76	Mid
	start-TVII	3039.85	0.55	3040.92	0.5	1.07	0.74	Mid
Stage 16	MIS 16	3051.95	0.55	3053.93	0.4	1.98	0.68	Low

Moisture source effects could cause the deuterium content to decrease earlier (hence deeper in the ice) than the associated CO₂ change. This may partially explain the disaccord between the modelled and observed Δ depth at the minimum before stage 14.3.

3 Results and discussion

3.1 800 ka history of $\delta^{18}\text{O}_{\text{atm}}$

The measured $\delta^{18}\text{O}_{\text{atm}}$ in EDC is in very good agreement with that measured in Vostok between 300 and 400 ka (overlap of 30 points EDC and 46 points Vostok, with $R^2=0.94$), as shown in Fig. 1. Both show variations between approximately 1.3 and -0.3‰ , with the ice volume signal becoming most apparent with the strong enrichments occurring several thousand years after glacial maxima. While the mean of measured $\delta^{18}\text{O}_{\text{atm}}$ is 0.39‰ for both Vostok over 0–400 ka and EDC over 300–800 ka, there is a small difference in median values with 0.38‰ for Vostok and 0.32‰ for EDC. This may, however, be due to the greater sample resolution for Vostok (mean 1300 years) compared to EDC (mean 3000 years), such that the strong enrichments associated with termina-

tions have a disproportionate effect on the EDC mean value. The highest $\delta^{18}\text{O}_{\text{atm}}$ enrichment of 1.48‰ is observed during Termination V (~ 425 ka). We note that the second and third most enriched $\delta^{18}\text{O}_{\text{atm}}$ values in the EDC record are associated with transitions from relatively cold to relatively warm conditions within interglacial stages 13 and 17 (with the $\delta^{18}\text{O}_{\text{atm}}$ maximum occurring 20 kyr after the cold period preceding 17.3). Glacial stage 16, which is highly enriched in the marine $\delta^{18}\text{O}_{\text{benthic}}$ stack (Lisiecki and Raymo, 2005) suggesting expansive ice sheets, is associated with only a relatively weak $\delta^{18}\text{O}_{\text{atm}}$ maximum of 0.97‰, although the low data resolution over this interval does not exclude our having missed the peak enrichment.

A period of very low $\delta^{18}\text{O}_{\text{atm}}$ variability (0.11‰ standard deviation compared to 0.34‰ for the entire 300 to 800 ka record) is notable between 710 and 780 ka, which corresponds to a period of low precession variability. This variability is still significant compared to the measurement precision of 0.028‰ for these samples, so that mid-slopes can still be determined for orbital tuning. Measurement precision also has implications for the choice of a control point at a shoulder in $\delta^{18}\text{O}_{\text{atm}}$ over the transition from stage 12 to 11. The difference between the two points defining the shoulder is 0.067‰, hardly significant compared to the 0.04‰ pooled

standard deviation for these data. A break in the slope of the transition is evident at this depth, supporting the presence of a shoulder despite the strong ice volume signal and low precession peak. Apart from these two regions of low precession variability, the determination of mid-slopes is unambiguous and preferable to correlating peaks given the 3000-year temporal resolution.

3.2 Confirmation of an age-scale anomaly

As discussed in the previous section, the 400 ka Vostok record showed that $\delta^{18}\text{O}_{\text{atm}}$ is characterised by strong coherence with mid-June 65° N insolation (Petit et al., 1999). The ice volume, hydrological cycle and productivity processes producing this signal are not expected to have varied in the preceding 400 kyr. Hence, the 40 kyr length of the cycle centred over stage 15.1 in the $\delta^{18}\text{O}_{\text{atm}}$ record on the EDC2 agescale is surprising. To determine whether this extended cycle is anomalous, we performed multi-taper method spectral analysis on comparable 80 kyr periods in the Vostok record, as well as on the precession parameter and the ShOTT composite precession and obliquity tuning target (Shackleton, 2000) over the same periods. As noted above, the global ice volume signal in $\delta^{18}\text{O}_{\text{atm}}$ is most pronounced at glacial terminations and could bias the analysis, so these periods are excluded. According to the marine LR04 $\delta^{18}\text{O}_{\text{benthic}}$ stack (Lisiecki and Raymo, 2005), glacial stage 14 and stage 15.2 do not appear to have been strongly glaciated, these periods are thus expected to show smaller $\delta^{18}\text{O}_{\text{atm}}$ enrichments than that observed for stage 12. In contrast to the strong 22 kyr periodicity found in the insolation curves and the $\delta^{18}\text{O}_{\text{atm}}$ of the four Vostok intervals (on the FGT1 timescale), EDC $\delta^{18}\text{O}_{\text{atm}}$ (on the EDC2 agescale) between 530 and 625 ka presents a 56 kyr cycle. This exceptional deviation from the precessional pacing is especially surprising given the large amplitude of variation in precession during this period (Fig. 1).

We conclude that the durations of stages 14 and 15.1 are too long by approximately a factor of two in the EDC2 chronology. While the deviation of $\delta^{18}\text{O}_{\text{atm}}$ from the expected relationship with precession is most notable over stages 14 and 15.1, close inspection of Figure 1a reveals several periods of incoherence, suggesting the presence of more agescale anomalies. There are indications of “skipped” precession cycles between stages 12 and 13, and again during stage 16. This reduced coherence with precession is visible in the low spectral power in the precession band of $\delta^{18}\text{O}_{\text{atm}}$ on EDC2 between 300–800 ka compared to Vostok over 0–400 ka (Fig. 3). These observations indicate that while the EDC2 agescale extends the duration of some intervals, it shortens the duration of others.

In the following sections, we use gas tracers and δD content of the ice to distinguish between accumulation and thinning as the source of the age-scale distortion, and we use orbital tuning of $\delta^{18}\text{O}_{\text{atm}}$ to define age control points that are used to constrain a correction function.

3.3 Chronological correction

We have derived a tuned timescale for the interval 2707.65–3189.8 m (398–802 ka) using a least squares method to minimize the age difference between $\delta^{18}\text{O}_{\text{atm}}$ -derived orbitally tuned control points (Table 1) and the corrected age scale:

$$A(z) = \int_0^z \frac{C(z')}{T(z')a(z')} dz' \quad (2)$$

where C is the best-fit correction factor for each depth. The method has been constructed to give a correction function that is close to 1, smooth, differentiable and continuous (see Appendix). We adjusted two parameters, smoothing length scale and regularity, to determine the optimum fit. Given a mean depth between age control markers of 13 m and a maximum separation of 34.7 m, we find that a smoothing length scale of 20 m is appropriate. Combined with a regularity factor of 0.5, this set of parameters results in a mean distance from control points of 0.9 kyr. Using length scales of 30 m and 10 m changes the mean distance from the control ages by 12.5 and –7.4%, respectively. Reducing the regularity was not found to reduce significantly the mean age difference.

The calculated correction factor is shown in Fig. 5b as $C(z)^{-1}$ such that a value greater than 1 represents compression of the original expected age scale, equivalent to either a positive accumulation anomaly or lower than expected thinning (larger thinning function). Over the corrected depth range, there are three intervals requiring compression of the EDC2 agescale by a factor of 1.5 to 2, compared to a longer interval of smaller amplitude expansion of the agescale between 2707 and 2865 m.

Previous studies have pointed out the exceptional durations of interglacial stages 11 (EPICA community members, 2004) and 15.1 (Siegenthaler et al., 2005). If we define an interglacial as a period when the temperature deviation from the mean of the last millennium is above -2.5°C , the duration of stage 11 on the corrected timescale is insignificantly longer than on the EDC2 agescale: 30 kyr on EDC2 versus 32 kyr on the corrected timescale. This is in contrast to the significantly reduced duration of stage 15.1 from 31 kyr to 16.4 kyr. The corrected agescale reduces the 2000 yr lead of CO₂ and CH₄ versus δD content at MIS 14.3 to a ~ 50 yr lag.

As one would expect given the tuning approach used, the corrected agescale restores power in the precession band of $\delta^{18}\text{O}_{\text{atm}}$, and, more interestingly, also shifts the peak power associated with obliquity into better agreement with the Vostok record (Fig. 3). We assess the influence of tuning exclusively to precession by repeating the above least-squares analysis using the same control points tied to ShOTT (Shackleton, 2000). The agescale correction agrees to within 2.6 kyr along the entire tuned section, with a mean difference of 0.6 kyr (ShOTT tuning older). Tuning $\delta^{18}\text{O}_{\text{atm}}$ to a record with a strong obliquity component does not significantly change the relative spectral power or peak frequency in the obliquity band.

Comparison of the δD record on the corrected chronology with the LR04 marine $\delta^{18}O_{\text{benthic}}$ stack (Lisiecki and Raymo, 2005) in Fig. 1 gives us confidence in the proposed agescale correction. Whereas the timing of climatic transitions differed by up to 20 kyr for the EDC2 chronology, the two records agree to within ± 5 kyr for the corrected chronology. We note that the tuning method used for LR04 and for the chronological correction involve different assumptions and tuning targets: an orbitally forced ice volume model for LR04 and the precession parameter for EDC.

As calculated above, the correction factor does not assume the source of the dating anomaly. In the next section we use in-situ Δ depth separating synchronous events recorded in CO₂ concentration and δD content of the ice to distinguish between accumulation and thinning as the source of the age-scale distortion.

3.4 Nature of the age-scale distortion

In Fig. 5c, modelled Δ depths for different scenarios of uncorrected, corrected assuming a pure thinning anomaly or corrected assuming anomalous accumulation are compared to the observed Δ depth separating synchronous events recorded in the gas and ice phases (Table 2). The Δ depth profiles of the previously uncorrected glaciological models (EPICA community members, 2004; Parrenin et al., 2007) show similar decreasing trends following the modelled thinning profile with low variability. The observed Δ depths, however, differ significantly from these modelled profiles around 2830, 2932 and 3000–3013 m, most notably for the peak of MIS 14.3 where the observed Δ depth of 7.22 ± 0.74 m is close to double the modelled Δ depth of 4.45 ± 0.9 m. While not perfect, the scenario assuming a pure thinning anomaly better captures the amplitude of these Δ depth variations (Fig. 5c, thick red line). In contrast, the scenario assuming anomalous accumulation fails to capture these features. This is not surprising as Δ depth is linearly dependent on the thinning function and only weakly dependent on the accumulation rate, as discussed in Sect. 2.3.

Additional physical and indirect arguments support a thinning over an accumulation anomaly. Precipitation in central Antarctica is deduced as a function of the condensation temperature, which can be estimated from the deuterium content of the snow (Jouzel et al., 1987). The 2-fold correction required over stages 14 to 15.1 implies an accumulation rate increase from 2.3 cm water equivalent yr⁻¹ to 5 cm w.e. yr⁻¹. Variations in the accumulation rate of up to 40% compared to the traditional accumulation-temperature-isotope relationship have been suggested by volcanic matching of EDC and Vostok (Udisti et al., 2004). A 100% change, however, would imply significant modifications in the moisture transport to central Antarctica and/or the thermodynamics controlling the inversion temperature over the site. No such changes are suggested from the deuterium excess record (Stenni et al., 2007). An additional indirect constraint on accumulation rate comes

in the form of flux profiles of chemical species measured in the ice. At low accumulation sites such as EDC, dry deposition is the dominant mechanism, so that measured concentrations must be corrected for accumulation rate to give fluxes. The 740 ka sulphate, calcium and sodium flux records show the same relationship to δD content both before and after 440 ka (Wolff et al., 2006), giving no indication of an accumulation anomaly. The distortion must then be mostly or entirely due to a flow anomaly.

From a material science point of view, ice is a polycrystalline material with a hexagonal structure. Due to the strong anisotropy of the ice crystal, c-axes rotate towards compressional axes and away from tensional axes (Azuma and Higashi, 1985). Under a dome, the ice experiences an uniaxial compression (Alley, 1988). This leads to the progressive formation of a vertical single maximum fabric along the EDC core (i.e. c-axes are clustered around the in-situ vertical) (Wang, 2003). However, below 2810 m, a sharp weakening of the fabric is observed in EDC as well as a tilting up to 20 degrees from the vertical of the fabric maximum. Moreover, the clustering of the fabric presents large fluctuation below this depths. No large, interlocking grains have been observed, suggesting that migration recrystallization is not affecting the fabric within the considered depth range. Thus, the fabric should still reflect the strain history experienced by the layers, and the observed anomaly in the fabric could be an indicator of strong flow disturbances.

It is difficult at this stage to find a scenario fully coherent with these observations. The corrected thinning profile indicates that the layer spanning 2920–3000 m has experienced approximately half as much thinning as expected. This could correspond to a stiffer layer that resists vertical compression. In this case, we would expect to see a clear correlation between fabric variations and the correction function, which we do not observe. Moreover, this scenario does not explain the tilt of the fabric orientation maximum. Another plausible scenario could be as follows: a layer presenting a well marked vertical single fabric is subjected to an horizontal compression, causing the c-axes to progressively rotate towards the horizontal. Such horizontal compression could account for lower than expected thinning, hence stretching in the age-scale. This is conceivable if the ice layer had to move up a hillside. This is not unrealistic considering that the dome at EDC may have moved in the past. The ice column beneath the dome coupled to this motion could then have been subjected to the effects of bedrock irregularities, which vary by up to 500 m within 50 km of the EDC drill site (Remy and Tabacco, 2000). We note that such a deformation would probably involve the ice column all the way from the bed up to a height more than double the topographic relief. While there are indications of anomalous flow over 500 m in the core, the deviation from the expected thinning profile varies in direction. Additional work is needed to understand the physical processes that are behind the observed heterogeneities, but this is beyond the scope of the present work.

Interpreting the correction function in terms of anomalous thinning has important implications for the flow around EDC. Firstly, the large amplitude and rapid changes in thinning are difficult to explain in steady state conditions, suggesting that non-steady state processes have occurred around Dome C. These could be due to dome movements, or to chaotic effects induced by feedbacks between the fabric and the ice flow, or both. Indeed, recent mechanical studies have shown that dust load can affect ice rheology (Durand et al., 2007). While this may play a role in the anomalous flow at EDC, it is likely not the main effect as there is no clear pattern between thinning anomaly and climate condition (with colder periods being associated with high dust concentrations).

Finally, we note that the correction was determined using control ages derived using $\delta^{18}\text{O}_{\text{atm}}$ tied to precession and converted to ice age controls using Δage . As noted above, Δage depends on accumulation rate but is almost independent of thinning. This is confirmed when the Δage calculated using the corrected agescale is compared to that using the uncorrected agescale and found to differ by less than 400 years.

4 Conclusions

Ice core age scales depend on the accumulation rate (parameterised as a function of site temperature) and strain rate (flow or thinning). While the physical constraints on ice flow generally imply that ice cores provide more reliable information on event duration than other sedimentary records, disturbances are known to occur, such as at the bottom of the Summit Greenland cores (Fuchs and Leuenberger, 1996; Grootes et al., 1993) and at Vostok (Raynaud et al., 2005). Here we have used the strong coherence between oxygen-18 of atmospheric O₂ and precession to confirm problems with the EDC2 agescale below 2700 m. Further, by comparing gas tracers and deuterium content of this ice we have determined that physical flow anomalies and not accumulation rate variations are responsible for the agescale distortion. Analysis of the ice fabric over the interval reveals perturbation in the crystal orientation consistent with anomalous flow.

Orbital tuning of $\delta^{18}\text{O}_{\text{atm}}$ and application of a least-squares method allows us to propose a corrected chronology with an accuracy of better than ± 6 kyr, and to derive a corrected thinning function. The duration of stage 15.1 is reduced by a factor of two in the corrected chronology, while the ~ 30 kyr duration of stage 11 is unchanged. As a consequence of these flow anomalies, the phasing between δD content and CO₂ concentration cannot be accurately determined at EDC prior to 400 ka.

This $\delta^{18}\text{O}_{\text{atm}}$ -derived correction is applied to a new glaciological chronology below 2700 m to give the new recommended agescale for EDC, EDC3, which will be fully described elsewhere (Parrenin et al., 2007b).

Limited understanding of the mechanisms controlling the phasing of $\delta^{18}\text{O}_{\text{atm}}$ response to ice volume changes and insolation forcing restrict the accuracy of the derived corrected chronology, however, new gas phase parameters, such as $\delta\text{O}_2/\text{N}_2$ and air content, both physically linked to local insolation variations (Bender, 2002), hold promise for further improving the chronology. Such improvements will enable the expected small deviations in phase of $\delta^{18}\text{O}_{\text{atm}}$ with respect to northern hemisphere summer insolation to be studied in detail, providing additional information on the O₂ cycle over the last 800 kyr.

Appendix A

We consider z_{min} and z_{max} the limits of the interval where the thinning function is corrected. We discretize the depth z and we denote $1, \dots, N$ the depth intervals of length Δz . In practice, we will use $\Delta z = 0.55$ m, i.e. each interval corresponds to a bag in the ice core. We further denote a_i the accumulation rate for each depth interval, and T_i its total thinning, as given by the 1-D ice flow model. The age at z_{min} is denoted A_0 , and the modelled age at the bottom of interval i is given by:

$$A_i^M = A_0 + \sum_{j=0}^i \frac{1}{a_j T_j} \quad (\text{A1})$$

We further modify the total thinning function by a correction factor $1/C_i$ for each interval, so that the corrected age is given by:

$$A_i^C = A_0 + \sum_{j=0}^i \frac{C_j}{a_j T_j} \quad (\text{A2})$$

We denote by A_k^D ($k=1, \dots, n_A$) the age markers given by the $\delta^{18}\text{O}_{\text{atm}}$ record for the bottom of the depth interval i_k .

The aim of the following least squares method is to find the correction function $C(z)$, with the following criteria: 1) C is as close as possible to 1; 2) the first and second derivatives, C' and C'' , are as small as possible (C is “smooth”); 3) C and C' are continuous at z_{min} and z_{max} ; and 4) the corrected age for interval i_k is as close as possible to A_k^D .

We thus try to minimize the following cost function:

$$F = F^R + F^{R1} + F^{R2} + F^C + F^A \quad (\text{A3})$$

$$F^R = \frac{1}{z_{\text{max}} - z_{\text{min}}} \sum_{i=0}^N \frac{(C_i - 1)^2}{(\sigma^R)^2} \Delta z \quad (\text{A4})$$

$$F^{R1} = \frac{1}{z_{\text{max}} - z_{\text{min}}} \sum_{i=0}^{N-1} \frac{((C_{i+1} - C_i) / \Delta z)^2}{(\sigma^{R1})^2} \Delta z \quad (\text{A5})$$

$$F^{R2} = \frac{1}{z_{\text{max}} - z_{\text{min}}} \sum_{i=0}^{N-2} \frac{((2C_i - C_{i+1} - C_{i-1}) / \Delta z^2)^2}{(\sigma^{R2})^2} \Delta z \quad (\text{A6})$$

$$F^C = \frac{(C_1 - 1)^2}{(\sigma^C)^2} + \frac{(C_2 - C_1)^2}{(\sigma^{C1})^2} + \frac{(C_N - 1)^2}{(\sigma^C)^2} + \frac{(C_N - C_{N-1})^2}{(\sigma^{C1})^2} \quad (\text{A7})$$

$$F^A = \frac{1}{n_A} \sum_{k=1}^{n_A} \frac{\left(\sum_{j=1}^{i_k} \frac{C_j}{a_j T_j} + A_0 - A_k^D \right)^2}{(\sigma_k^A)^2} \quad (\text{A8})$$

For the continuity of C and C' , σ^C and σ^{C1} are taken as small quantities.

σ^R represents the typical misfit expected between C and 1. To evaluate the values of σ^{R1} and σ^{R2} , we perform a harmonic analysis, considering C as a sinusoidal function of depth:

$$C(z) = 1 + \Delta C_0 \sin\left(\pi \frac{z}{L}\right) \quad (\text{A9})$$

C' and C'' are respectively given by:

$$C'(z) = 1 + \frac{\pi}{L} \Delta C_0 \cos\left(\pi \frac{z}{L}\right) \quad (\text{A10})$$

$$C''(z) = 1 - \left(\frac{\pi}{L}\right)^2 \Delta C_0 \sin\left(\pi \frac{z}{L}\right) \quad (\text{A11})$$

We deduce that $\sigma^R = \Delta C_0$ and the values of σ^{R1} and σ^{R2} can be derived from σ^R and the typical smoothing wavelength L as:

$$\sigma^{R1} = \sigma^R \frac{\pi}{L} \quad (\text{A12})$$

$$\sigma^{R2} = \sigma^R \left(\frac{\pi}{L}\right)^2 \quad (\text{A13})$$

In practice, we used $\sigma^R=0.5$ and $L=20$ m. See text for discussion of parameter choice.

Acknowledgements. This work is a contribution to the European Project for Ice Coring in Antarctica (EPICA), a joint European Science Foundation/European Commission scientific programme, funded by the EU (EPICA-MIS) and by national contributions from Belgium, Denmark, France, Germany, Italy, the Netherlands, Norway, Sweden, Switzerland and the UK. The main logistic support was provided by IPEV and PNRA (at Dome C) and AWI (at Dronning Maud Land). Additional funding was provided by the French Agence Nationale de la Recherche (PICC project). We thank B. Minster, M. Stievenard, S. Falourd and O. Cattani for technical support. This is EPICA publication no. 171.

Edited by: T. van Ommen

References

- Alley, R. B.: Fabrics in polar ice sheets: development and prediction, *Science*, 240, 493–495, 1988.
- Azuma, N. and Higashi, A.: Formation processes of ice fabric pattern in ice sheets, *Ann. Glaciol.*, 6, 130–134, 1985.
- Bender, M., Sowers, T., Dickson, M. L., Orchado, J., Grootes, P., Mayewski, P. A., and Meese, D. A.: Climate correlations between Greenland and Antarctica during the last 100 000 years, *Nature*, 372, 663–666, 1994a.
- Bender, M., Sowers, T., and Labeyrie, L. D.: The Dole effect and its variation during the last 130 000 years as measured in the Vostok core, *Global Biogeochem. Cy.*, 8, 363–376, 1994b.
- Bender, M. L.: Orbital tuning chronology for the Vostok climate record supported by trapped gas composition, *Earth Planet. Sci. Lett.*, 204, 275–289, 2002.
- Bintanja, R., van de Wal, R. S. W., and Oerlemans, J.: Modelled atmospheric temperatures and global sea levels over the past million years, *Nature*, 437, 125–128, 2005.
- Brook, E. J., Sowers, T., and Orchado, J.: Rapid variations in atmospheric methane concentration during the past 110 000 years, *Science*, 273, 1087–1090, 1996.
- Caillon, N., Severinghaus, J. P., Jouzel, J., Barnola, J.-M., Kang, J., and Lipenkov, V. Y.: Timing of atmospheric CO₂ and Antarctic temperature changes across Termination III, *Science*, 299, 1728–1731, 2003.
- Cuffey, K. M. and Vimeux, F.: Covariation of carbon dioxide and temperature from the Vostok ice core after deuterium-excess correction, *Nature*, 412, 523–527, 2001.
- Durand, G., Gillet-Chaulet, F., Svensson, A., Gagliardini, O., Kipfstuhl, J., Meyssonier, J., Parrenin, F., Duval, P., and Dahl-Jensen, D.: Change of the ice rheology with climatic transitions – implication on ice flow modelling and dating of the EPICA Dome C core, *Clim. Past*, 3, 155–167, 2007, <http://www.clim-past.net/3/155/2007/>.
- EPICA community members: 8 Glacial cycles from an Antarctic ice core, *Nature*, 429, 623–628, 2004.
- Fischer, H., Wahlen, M., Smith, J., Mastroianni, D., and Deck, B.: Ice Core Records of Atmospheric CO₂ Around the Last Three Glacial Terminations, *Science*, 283, 1712–1714, 1999.
- Fuchs, A. and Leuenberger, M. C.: $\delta^{18}\text{O}$ of atmospheric oxygen measured on the GRIP ice core document stratigraphic disturbances in the lowest 10% of the core, *Geophys. Res. Lett.*, 23, 1049–1052, 1996.
- Goujon, C., Barnola, J.-M., and Ritz, C.: Modeling the densification of polar firn including heat diffusion: Application to close-off characteristics and gas isotopic fractionation for Antarctica and Greenland sites, *J. Geophys. Res.*, 108, 4792, doi:10.1029/2002JD003319, 2003.
- Grootes, P. M., Stuiver, M., White, J. W. C., Johnsen, S. J., and Jouzel, J.: Comparison of the oxygen isotope records from the GISP2 and GRIP Greenland ice cores, *Nature*, 366, 552–554, 1993.
- Hoffmann, G., Cuntz, M., Weber, C., Ciais, P., Friedlingstein, P., Heimann, M., Jouzel, J., Kaduk, J., Maier-Reimer, E., Seibt, U., and Six, K.: A model of the Earth's Dole effect, *Global Biogeochem. Cy.*, 18, GB1008, doi:10.1029/2003GB002059, 2004.
- Huber, C. and Leuenberger, M.: Measurements of isotope and elemental ratios of air from polar ice with a new on-line extraction method, *Geochem. Geophys. Geosyst.*, 5, Q10002,

- doi:10.1029/2004GC000766, 2004.
- Huber, C., Leuenberger, M., and Zumbrennen, O.: Continuous extraction of trapped air from bubble ice or water for on-line determination of isotope ratios, *Anal. Chem.*, 75, 2324–2332, 2003.
- Jouzel, J., Hoffmann, G., Parrenin, F., and Waelbroeck, C.: Atmospheric oxygen 18 and sea-level changes, *Quaternary Sci. Rev.*, 21, 307–314, 2002.
- Jouzel, J., Lorius, C., Petit, J. R., Genthon, C., Barkov, N. I., Kotlyakov, V. M., and Petrov, V. M.: Vostok ice core: a continuous isotope temperature record over the last climatic cycle (160 000 years), *Nature*, 329, 403–408, 1987.
- Jouzel, J., Waelbroeck, C., Malaizé, B., Bender, M., Petit, J. R., Stievenard, M., Barkov, N. I., Barnola, J. M., King, T., Kotlyakov, V. M., Lipenkov, V., Lorius, C., Raynaud, D., Ritz, C., and Sowers, T.: Climatic interpretation of the recently extended Vostok ice records, *Clim. Dynam.*, 12, 513–521, 1996.
- Landais, A., Caillon, N., Severinghaus, J., Jouzel, J., and Masson-Delmotte, V.: Analyses isotopiques à haute précision de l'air piégé dans les glaces polaires pour la quantification des variations rapides de température: méthode et limites, *Notes des Activités Instrumentales de l'IPSL*, Note no. 39, 2003a.
- Landais, A., Chappellaz, J., Delmotte, M., Jouzel, J., Blunier, T., Bour, C., Caillon, N., Cherrier, S., Malaizé, B., Masson-Delmotte, V., Raynaud, D., Schwander, J., and Steffensen, J. P.: A tentative reconstruction of the last interglacial and glacial inception in Greenland based on new gas measurements in the Greenland Ice Core Project (GRIP) ice core, *J. Geophys. Res.*, 108, 4563, doi:10.1029/2002JD003147, 2003b.
- Laskar, J., Robutel, P., Joutel, F., Gastineau, M., Correia, A. C. M., and Levrard, B.: A long-term numerical solution for the insolation quantities of the Earth, *A&A*, 428, 261–285, 2004.
- Leuenberger, M. C.: Modeling of the signal transfer of seawater $\delta^{18}\text{O}$ to the $\delta^{18}\text{O}$ of atmospheric oxygen using a diagnostic box model for the terrestrial and marine biosphere, *J. Geophys. Res.*, 102, 26 841–26 850, 1997.
- Lisiecki, L. E. and Raymo, M. E.: A Pliocene-Pleistocene stack of 57 globally distributed benthic $\delta^{18}\text{O}$ records, *Paleoceanography*, 20, PA1003, doi:10.1029/2004PA001071, 2005.
- Malaizé, B., Paillard, D., Jouzel, J., and Raynaud, D.: The Dole effect over the last two glacial-interglacial cycles, *J. Geophys. Res.*, 104, 14 199–14 208, 1999.
- Meese, D. A., Gow, A. J., Alley, R. B., Grootes, P., Ram, M., Taylor, K. C., Zielinski, G. A., Bolzan, J. F., Mayewski, P. A., and Waddington, E. D.: The accumulation record from the GISP2 core as an indicator of climate change throughout the Holocene, *Science*, 266, 1680–1682, 1994.
- Monnin, E., Indermuhle, A., Dallenbach, A., Flückiger, J., Stauffer, B., Stocker, T. F., Raynaud, D., and Barnola, J.-M.: Atmospheric CO₂ Concentrations over the Last Glacial Termination, *Science*, 291, 112–114, 2001.
- Paillard, D., Labeyrie, L. D., and Yiou, P.: Macintosh program performs time-series analysis, *EoS Trans. AGU*, 77, 379, 1996.
- Parrenin, F., Jouzel, J., Waelbroeck, C., Ritz, C., and Barnola, J.-M.: Dating the Vostok ice core by an inverse method, *J. Geophys. Res.*, 106, 31 837–31 851, 2001.
- Parrenin, F., Rémy, F., Ritz, C., Siegert, M. J., and Jouzel, J.: New modelling of the Vostok ice flow line and implication for the glaciological chronology of the Vostok ice core, *J. Geophys. Res.*, 109, D20102, doi:10.1029/2004JD004561, 2004.
- Parrenin, F., Dreyfus, G., Durand, G., Fujita, S., Gagliardini, O., Gillet, F., Jouzel, J., Kawamura, K., Lhomme, N., Masson-Delmotte, V., Ritz, C., Schwander, J., Shoji, H., Uemura, R., Watanabe, O., and Yoshida, N.: Ice flow modelling at EPICA Dome C and Dome Fuji, East Antarctica, *Clim. Past*, 3, 243–259, 2007a.
- Parrenin, F., Barnola, J.-M., Beer, J., Blunier, T., Castellano, E., Chappellaz, J., Dreyfus, G., Fischer, H., Fujita, S., Jouzel, J., Kawamura, K., Lemieux-Dudon, B., Loulergue, L., Masson-Delmotte, V., Narcisi, B., Petit, J. R., Raisbeck, G., Raynaud, D., Ruth, U., Schwander, J., Severi, M., Spahni, R., Steffensen, J. P., Svensson, A., Udisti, R., Waelbroeck, C., and Wolff, E. W.: The EDC3 chronology for the EPICA Dome C ice core, *Clim. Past Discuss.*, 3, 575–606, 2007b.
- Petit, J. R., Jouzel, J., Raynaud, D., Barkov, N. I., Barnola, J. M., Basile, I., Bender, M., Chappellaz, J., Davis, M., Delaygue, G., Delmotte, M., Kotlyakov, V. M., Lorius, C., Pepin, L., Ritz, C., Saltzman, E., and Stievenard, M.: Climate and atmospheric history of the past 420 000 years from the Vostok ice core, Antarctica, *Nature*, 399, 429–436, 1999.
- Prell, W. L. and Kutzbach, J.: Monsoon variability over the past 150,000 years, *J. Geophys. Res.*, 92, 8411–8425, 1987.
- Rasmussen, S. O., Andersen, K. K., Svensson, A. M., Steffensen, J. P., Vinther, B. M., Clausen, H. B., Siggaard-Andersen, M. L., Johnsen, S. J., Larsen, L. B., Dahl-Jensen, D., Bigler, M., Röthlisberger, R., Fischer, H., Goto-Azuma, K., Hansson, M. E., and Ruth, U.: A new Greenland ice core chronology for the last glacial termination, *J. Geophys. Res.-Atmos.*, 111, D06102, doi:10.1029/2005JD006079, 2006.
- Raynaud, D., Barnola, J. M., Souchez, R., Lorrain, R., Petit, J. R., Duval, P., and Lipenkov, V. I.: The record for marine isotopic stage 11, *Nature*, 436, 39–40, 2005.
- Remy, F. and Tabacco, I. E.: Bedrock features and ice flow near the EPICA ice core site (Dome C, Antarctica), *Geophys. Res. Lett.*, 27, 405–408, 2000.
- Shackleton, N. J.: The 100 000-Year Ice-Age Cycle Identified and Found to Lag Temperature, Carbon Dioxide, and Orbital Eccentricity, *Science*, 289, 1897–1902, 2000.
- Siegenthaler, U., Stocker, T. F., Monnin, E., Luthi, D., Schwander, J., Stauffer, B., Raynaud, D., Barnola, J.-M., Fischer, H., Masson-Delmotte, V., and Jouzel, J.: Stable Carbon Cycle-Climate Relationship During the Late Pleistocene, *Science*, 310, 1313–1317, 2005.
- Sowers, T., Bender, M., Raynaud, D., Korotkevich, Y. S., and Orchardo, J.: The $\delta^{18}\text{O}$ of atmospheric O₂ from air inclusions in the Vostok ice core: timing of CO₂ and ice volume change during the penultimate deglaciation, *Paleoceanogr.*, 6, 679–696, 1991.
- Sowers, T., Brook, E., Etheridge, D., Blunier, T., Fuchs, A., Leuenberger, M., Chappellaz, J., Barnola, J. M., Wahlen, M., Deck, B., and Weyhenmeyer, C.: An interlaboratory comparison of techniques for extracting and analyzing trapped gases in ice cores, *J. Geophys. Res.*, 102, 26 527–26 538, 1997.
- Spahni, R., Chappellaz, J., Stocker, T. F., Loulergue, L., Hausamann, G., Kawamura, K., Flückiger, J., Schwander, J., Raynaud, D., Masson-Delmotte, V., and Jouzel, J.: Atmospheric methane and nitrous oxide of the Late Pleistocene from Antarctic ice cores, *Science*, 310, 1317–1321, 2005.
- Stenni, B., Selmo, E., Masson-Delmotte, V., Jouzel, J., Braida, M., Cattani, O., Falourd, S., Iacumin, P. and Johnsen, S. J.: A 800

- ky deuterium excess record from the EPICA Dome C ice core, *Geophys. Res. Abstr.*, 9, 03238, 2007.
- Suwa, M., von Fischer, J. C., Bender, M. L., Landais, A., and Brook, E. J.: Chronology reconstruction for the disturbed bottom section of the GISP2 and the GRIP ice cores: Implications for Termination II in Greenland, *J. Geophys. Res.*, 111, D02101, doi:10.1029/2005JD006032, 2006.
- Udisti, R., Becagli, S., Castellano, E., Delmonte, B., Jouzel, J., Petit, J. R., Schwander, J., Stenni, B., and Wolff, E. W.: Stratigraphic correlations between the European Project for Ice Coring in Antarctica (EPICA) Dome C and Vostok ice cores showing the relative variations of snow accumulation over the past 45 kyr, *J. Geophys. Res.*, 109, D08101, doi:10.1029/2003JD004180, 2004.
- Wang, Y., Kipfstuhl, S., Azuma, N., Thorsteinsson, T., and Miller, H.: Ice-fabrics study in the upper 1500 m of the Dome C (East Antarctica) deep ice core, *Ann. Glaciol.*, 37, 97–104, 2003.
- Wolff, E. W., Fischer, H., Fundel, F., Ruth, U., Twarloh, B., Littot, G. C., Mulvaney, R., Rothlisberger, R., de Angelis, M., Boutron, C. F., Hansson, M., Jonsell, U., Hutterli, M. A., Lambert, F., Kaufmann, P., Stauffer, B., Stocker, T. F., Steffensen, J. P., Bigler, M., Siggaard-Andersen, M. L., Udisti, R., Becagli, S., Castellano, E., Severi, M., Wagenbach, D., Barbante, C., Gabrielli, P., and Gaspari, V.: Southern Ocean sea-ice extent, productivity and iron flux over the past eight glacial cycles, *Nature*, 440, 491–496, 2006.